C−H Activation of Ethane by Group 4 Metal Atoms: Observation and Characterization of the $MH-CH_2CH_3$, $MH_2-(CH_2)_2$, and $MH_3-CH=CH_2$ Complexes

Han-Gook Cho and Lester Andrews*

Department of Chemistry, University of Incheon, 177 Dohwa-dong, Nam-ku, Incheon, 402-749, South Korea and Department of Chemistry, University of Virginia, P.O. Box 400319, Charlottesville, Virginia 22904-4319

Received: September 25, 2007; In Final Form: October 30, 2007

Group 4 metal atoms excited in the laser ablation process activate ethane to form the C−H insertion product, the metallacyclopropane dihydride, and vinyl metal trihydride complexes as major products. These three new metal hydrides are characterized by their strong M−H stretching absorptions and other weaker modes as predicted by density functional theory vibrational frequency calculations.

Introduction

High oxidation state complexes containing a carbon−transition metal double bond are important for understanding metal coordination and exploring catalyst systems to be used in alkene metatheses and alkane activation.[1−5] Many early transition-metal alkylidenes are agostic, and these species provide a means to characterize the agostic interaction of hydrogen to a transition-metal center and help understand the important C−H activation process. Agostic bonding in these compounds involves α-H-to-metal interaction and stabilization of the C=M double bond,[6−9] and the simplest methylidene model systems made by methane activation can contribute to understand this bonding interaction through detailed quantum chemical calculations.[10]

In this laboratory we have explored a new generation of simple methylidene complexes prepared by reaction of excited early transition-metal atoms with methane during condensation in excess argon.[11−14] The methane (a) reaction mechanism goes first through the basic C−H insertion step (1a) followed by one α-H transfer to the metal center to form the methylidene (2a), as shown in Scheme 1. The transfer of a second α-H to the metal center to give the unstable trihydride (3a) is highly endothermic for group 4 metal atoms, but the heavier group 6 metal atoms readily form methylidyne trihydride complexes.[15,16]

We now wish to explore these reactions and their various complex products using instead the ethane reagent, reactions b and c. One immediately finds two insertion possibilities, C−H (1b) and C−C (1c) in Scheme 1, followed by α-H-transfer to give two different ethylidene complexes (2b and 2c). In the first case, following C−H insertion the trihydride product is stabilized by the larger vinyl group (3b), and this product is now competitive energy wise. In addition, β-H transfer (from 1b) facilitates the metallacyclopropane dihydride (2β), which is also stable. The latter complex was investigated theoretically for second-row transition-metal atoms, and this zirconium dihydride was found to be the most stable reaction product.[17] In the second case, insertion into the C−C bond followed by α-H transfers leads to isomeric products. We wish to calculate the relative stability of these possible products for each of the subject metals and identify the reaction products from their infrared spectra.

SCHEME 1

$$M + CH_4 \rightarrow \underset{1a}{CH_3{-}MH} \rightarrow \underset{2a}{CH_2{=}MH_2} \rightarrow \underset{3a}{CH{-}MH_3} \quad (a)$$

$$M + C_2H_6 \rightarrow \underset{1b}{CH_3CH_2{-}MH} \rightarrow \underset{2b}{CH_3(H)C{=}MH_2} \rightarrow \underset{3b}{CH_2{=}CH{-}MH_3} \quad (b)$$

$$M + C_2H_6 \rightarrow \underset{1c}{CH_3{-}M{-}CH_3} \rightarrow \underset{2c}{CH_2{=}M(H)CH_3} \rightarrow \underset{3c}{CH{-}M(H)_2CH_3} \quad (c)$$

$(CH_2)_2{-}MH_2$

2β

Experimental and Theoretical Methods

Our experimental design has been described previously.[18,19] Metal atoms, produced by ablation with a Nd:YAG laser, were co-deposited with a dilute mixture (1−2%) of reagent vapor (C_2H_6, Matheson; C_2D_6, MSD Isotopes) in argon onto a CsI window cooled to 8 K. The resulting reaction products were frozen in the argon matrix so formed, and the infrared spectrum was recorded on a Nicolet 550 spectrometer. Matrix samples were irradiated for 20 min periods by a medium-pressure mercury arc street lamp with the globe removed ($\lambda > 220$ nm) with or without optical glass filters and subsequently annealed to various temperatures. Additional infrared spectra were recorded following each procedure.

Theoretical calculations on possible reaction products were performed using the Gaussian 03 program system.[20] In all instances, the B3LYP hybrid density functional was employed.[21] Carbon and hydrogen atoms were given the large 6-311++G-(3df,3pd) Gaussian basis, titanium atoms the all-electron Wachters−Hay set, and Zr and Hf metal centers the SDD pseudopotential and valence basis sets.[22−24] Such DFT calculations predict vibrational frequencies with reasonable accuracy for transition-metal compounds.[14−16] Unscaled frequencies are reported to the nearest 0.1 cm^{-1}, not for absolute accuracy, but for precise determination of the mechanical isotopic shifts. Geometries were fully relaxed during optimization, and the stable minimum-energy structure was confirmed by vibrational analysis. Anhar-

* To whom correspondence should be addressed. E-mail: lsa@virginia.edu.

10.1021/jp077704g CCC: $40.75
Published on Web 01/25/2008

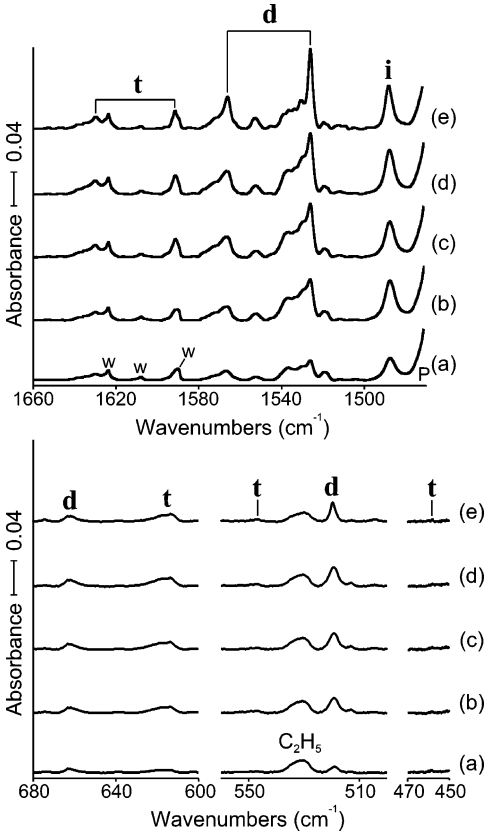

Figure 1. IR spectra in the regions of 1660−1470, 680−600, 560−500, and 470−450 cm^{-1} for laser-ablated Zr atoms co-deposited with C_2H_6 in excess argon at 8 K. (a) Zr + 1.0% C_2H_6 in Ar co-deposited for 1 h. (b) As in a after photolysis (λ > 420 nm). (c) As in b after photolysis (240 < λ < 380 nm). (d) As in c after photolysis (λ > 420 nm). (e) As in d after annealing to 28 K. **i**, **d**, and **t** denote the product absorption groups.

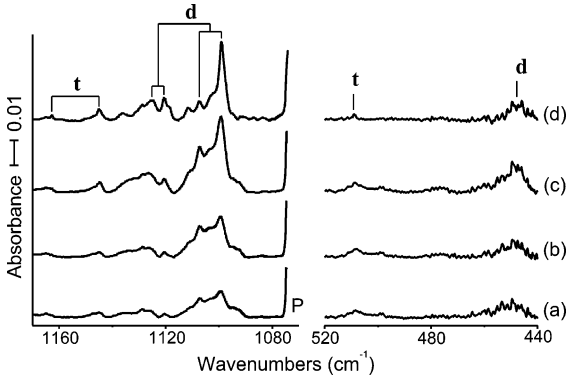

Figure 2. IR spectra in the regions of 1170−1070 and 520−440 cm^{-1} for laser-ablated Zr atoms co-deposited with C_2D_6 in excess argon at 8 K. (a) Zr + 1.0% C_2D_6 in Ar co-deposited for 1 h. (b) As in a after photolysis (λ > 420 nm). (c) As in b after photolysis (240 < λ < 380 nm). (d) As in c after annealing to 28 K. **i**, **d**, and **t** denote the product absorption groups.

TABLE 1: Observed and Calculated Harmonic Frequencies of New Product Absorptions from Reactions of Ethane Molecules with Zr Atoms in Excess Argon[a]

	C_2H_6		C_2D_6		
	obsd	calcd	obsd	calcd	description
i	1487.7	1600.0 (405)	b	1138.3 (206)	Zr−H str.
	504.3	538.8 (70)		434.1 (51)	C−Zr str.
d	1566.1	1626.8 (385)	1120.5	1154.2 (197)	A_1 ZrH_2 str.
	958.8	993.2 (25)		853.7 (16)	A_1 CC str.
	662.6	666.6 (81)		499.1 (56)	A_1 ZrH_2 scis.
	1526.1	1591.2 (698)	1099.2	1136.2 (360)	B_1 ZrH_2 str.
	925.0	960.7 (20)		809.6 (3)	B_2 CH_2 wag
	519.5	519.7 (119)	448.4	451.8 (82)	B_2 ZrC_2 str.
t	1629.9	1695.6 (213)	1162.9	1201.8 (111)	A ZrH_3 str.
	1591.2	1646.0 (542)	1144.9	1172.6 (289)	A ZrH_3 str
	618.3	620.5 (280)	508.6	520.6 (122)	A ZrH_3 deform
	547.0	594.9 (60)		422.6 (32)	A ZrH_3 scis.
	1596.1	1655.1 (488)	1147.2	1180.3 (254)	A ZrH_3 str.
	458.6	485.8 (82)		368.5 (45)	A ZrH_3 rock

[a] All frequencies are in cm^{-1}. Observed in argon matrix. Description gives major coordinates. **i**, **d**, and **t** stand for insertion, dihydrido, and trihydrido products, respectively. Harmonic frequencies calculated with B3LYP/6-311++G(3df,3pd)/SDD are not scaled. [b] Covered by precursor absorption.

monic frequency calculations by numerical differentiation[25] (with Gaussian 03 keyword anharmonic) were also carried out with B3LYP to compare with experimental values and examine the effects of anharmonicity. Harmonic MP2 calculations[26] were also done to support the B3LYP results. Zero-point energy is included for calculation of the binding energy for a metal complex.

Results and Discussion

New product absorptions in laser-ablated group 4 metal atom reactions with ethane will be compared with frequencies calculated for the most stable products in these systems. Ethane photolysis products such as methane, ethylene, and ethyl radical are common to our laser ablation experiments.[11−16,27,28]

Zr + Ethane. Shown in Figures 1 and 2 are IR spectra from the reactions of laser-ablated Zr atoms with C_2H_6 and C_2D_6. Three sets of product absorptions marked with **i**, **d**, and **t** (for monohydride insertion product and dihydride and trihydride species) are observed and grouped on the basis of their behaviors upon photolysis and annealing, and the observed frequencies are summarized in Table 1. The isolated ethyl radical photolysis product absorption is observed here at 531 cm^{-1}.[28] The three sets of product absorptions are clearly noticeable in the original spectra after deposition. The **i** and **d** absorptions almost double on visible (λ > 420 nm) photolysis, while the **t** absorptions increase only slightly. The **i** absorption decreases slightly (~10% of the original intensity) on subsequent UV (240 < λ < 360 nm) photolysis, while the **d** absorptions increase another 70% and the **t** absorptions double. The **i** absorption increases about 20% on the second visible photolysis, whereas the **d** and **t** absorptions increase another ~30% (about 110%, 200%, and 130% increases in total for **i**, **d**, and **t** absorptions, respectively). The product absorptions sharpen in the following annealing and decrease on higher annealings.

In the original spectra, the **i** absorption at 1487.7 cm^{-1} is the strongest, but due to the large increases on photolysis and sharpening on annealing, the **d** absorptions eventually appear most prominent, particularly, in the Zr−H stretching region.[29] The observed three sets of product absorptions are believed to originate from the three major products formed in the reaction of Zr atoms with ethane. The strong Zr−H stretching absorptions observed in the 1660−1470 cm^{-1} region in the C_2H_6 spectra and in the 1170−1070 cm^{-1} region in the C_2D_6 spectra show that C−H insertion by Zr atoms occurs readily in reaction of Zr atoms with ethane and further rearrangements also follow. The high intensity of the **i** absorption at 1487.7 cm^{-1} in the original spectrum and dramatic increases of the **d** and **t** absorptions on photolysis afterward suggest that a product responsible for the single **i** absorption is first formed in the reaction of Zr with ethane and the other two products responsible

for the **d** and **t** absorptions are formed subsequently or on photolysis afterward.

The single strong **i** absorption at 1487.7 cm^{-1} suggests that it originates from a product with a single Zr−H bond; however, its deuterium counterpart is unfortunately covered by a precursor absorption. The relatively low frequency is consistent with the tendency that the hydrogen stretching frequency increases with the number of Zr−H bonds.[29] The most probable product is $H-Zr-CH_2CH_3$, the complex formed by insertion of Zr into a C−H bond. Another **i** absorption at 504.3 cm^{-1} is assigned to the C−Zr stretching mode without observation of the deuterium counterpart, which is expected near 400 cm^{-1}, below our observation limit. The predicted frequencies and intensities of $ZrH-CH_2CH_3$ listed in Table S1 show that the Zr−H stretching band is predominantly strong, and remaining absorptions are much weaker other than the C−Zr stretching band.

Previous studies show that the insertion complex is first formed in reaction of metal atoms with methane and methyl halides, and the dihydride and trihydrido products are also generated via α-hydrogen migration during deposition or photolysis and annealing afterward.[11−16] The distinctive two strong absorptions at 1566.1 and 1526.1 cm^{-1} with about 1:2 intensity ratio have their deuterium counterparts at 1120.5 and 1099.2 cm^{-1} (H/D ratios of 1.398 and 1.388, respectively). The frequencies are also compared with the previously reported Zr−H stretching frequencies of 1518.6, 1545.3, and 1623.6 cm^{-1} for ZrH_2, ZrH_3, and ZrH_4 and the Zr−D stretching frequencies of 1092.5, 1110.3, and 1166.6 cm^{-1} for ZrD_2, ZrD_3, and ZrD_4, respectively.[29] The zirconium hydride absorptions including the diatomic ZrH and ZrD bands at 1540.8 and 1104.5 cm^{-1} are not observed in this study.

Therefore, the two Zr−H stretching absorptions for species **d** with a 1:2 intensity ratio most likely arise from a major reaction product containing a ZrH_2 group. Calculations show that the two most plausible products with a ZrH_2 group from the reaction of Zr with ethane are zirconium metallapropane dihydride ($ZrH_2-(CH_2)_2$) and zirconium methyl methylidene dihydride ($ZrH_2=CHCH_3$). The latter $ZrH_2=CHCH_3$ can be formed via α-hydrogen migration from the insertion complex ($ZrH-CH_2CH_3$), analogous to the methylidene complexes,[11−16] whereas $ZrH_2-(CH_2)_2$ requires *β*-hydrogen migration. Although the Zr···H(α) distance (2.685 Å) is shorter than the Zr···H(*β*) distance (3.358 Å), the cyclic product is considerably more stable (20 kcal/mol) than the methylidene product.

In addition, the observed frequencies are in much better agreement with the predicted values for $ZrH_2-(CH_2)_2$ than those for $ZrH-CH_2CH_3$ shown in Tables S2 and S4, respectively. Particularly, the low-frequency **d** absorptions at 662.6 and 519.5 cm^{-1} show a good match with the predicted values for the ZrH_2 scissoring and ZrC_2 stretching modes (666.6 and 519.7 cm^{-1}) of the metallacyclic product. On the other hand, the methylidene complex would not have observable absorptions in this frequency region as shown in Table S4. The weak **d** absorptions at 958.8 and 925.0 cm^{-1} (not shown) are tentatively assigned to the A_1 C−C stretching and B_2 CH_2 wagging modes of $ZrH_2-(CH_2)_2$ without observation of the D counterparts.

Formation of $ZrH_2-(CH_2)_2$ is somewhat surprising; in reactions of metal atoms with methane and methyl halides, the methylidene ($CH_2=MHX$, X = H or halogen) is typically the major product.[11−16] However, in the Zr + C_2H_6 system, the Zr metallocycle is the most stable plausible product,[17] which is consistent with the highest intensity of the **d** absorptions. In addition, calculations also suggest that the *β*-hydrogen migration is energetically more favored in the reaction with ethane than

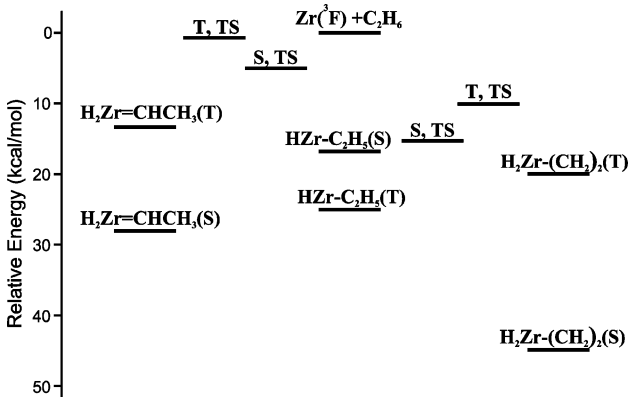

Figure 3. Relative energies of transition states between the H−Zr−CH_2CH_3 insertion product and the most stable Zr metallacyclic product, $ZrH_2-(CH_2)_2$ and the methylidene complex, $ZrH_2=CHCH_3$. S and T indicate singlet and triplet states, and TS denotes transition state. Energies from B3LYP calculations.

the α-hydrogen migration as the singlet and triplet transition states between the insertion and cyclic products are 9−10 kcal/mol lower than those between the insertion and the methylidene products as shown by the energy profile diagram in Figure 3. The stability of the metallacyclic product, good agreement between the observed and predicted frequencies, and expected easier *β*-hydrogen migration together substantiate formation of $ZrH_2-(CH_2)_2$. The present experimental agreement is typical of that found with harmonic frequencies computed by density functional theory.[30] Notice, however, that the anharmonic calculated Zr−H stretching frequencies better approximate the observed frequencies (Tables S1−S3) as such vibrations of light atoms have substantial anharmonic character.

In the Zr−H stretching region, the **t** absorptions are the weakest and the frequencies are the highest. The absorptions at 1629.9 and 1591.2 cm^{-1} have their D counterparts at 1162.9 and 1144.9 cm^{-1} (H/D ratios of 1.402 and 1.390). The next associated band at 1596.1 cm^{-1} shifts to 1147.2 cm^{-1} with deuterium (H/D ratio 1.391). The high frequencies and observation of three associated Zr−H stretching modes suggest that the **t** absorptions arise from a product with three Zr−H bonds. The most energetically conceivable additional product is $ZrH_3-CH=CH_2$, which is only 4.2 kcal/mol higher in energy than $ZrH_2-(CH_2)_2$, and the observed frequencies are compared with the predicted frequencies for the trihydrido complex in Tables 1 and S3, which are again in very good agreement.

$ZrH_3-CH=CH_2$ has the C_s structure in its singlet ground state. The **t** absorption at 618.3 cm^{-1} has its D counterpart at 508.6 cm^{-1} (H/D ratio of 1.22) and is attributed to the A′ ZrH_3 deformation mode. The observed absorptions at 547.0 and 458.6 cm^{-1} are assigned to the A′ ZrH_3 scissoring and A″ ZrH_3 rocking modes, respectively. The D counterparts are beyond our observation limit (too low in frequency).

In a recent study, a trihydrido Zr complex (ZrH_3-CCH) was prepared along with $ZrH-CH=CH_2$ and $ZrH_2-(CH)_2$ in the reaction of Zr atoms with ethylene.[27] It turns out that the trihydrido complex is energetically comparable with the dihydrido product, $ZrH_2-(CH)_2$, and calculations show that they are easily interconvertible. The present result, therefore, reconfirms that a trihydrido Zr complex is easily generated via hydrogen migration from a dihydrido Zr complex, regardless of the presence of *π* electrons. It is interesting to note the trihydride $HCZrH_3$ is too high in energy to be formed in the methane system;[12] hence, the stabilization afforded by the vinyl substituent makes the present trihydride species competitive.

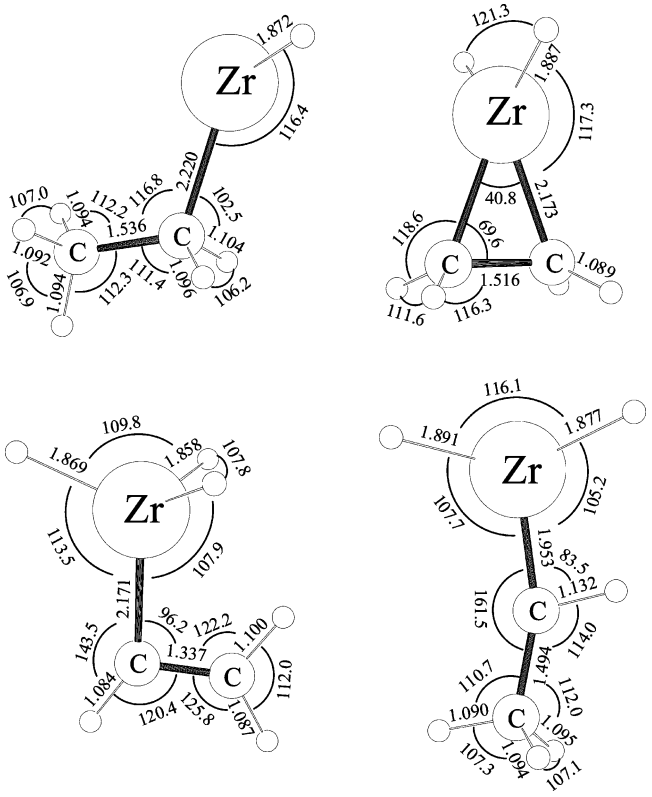

Figure 4. Structures of $ZrH-CH_2CH_3$, $ZrH_2-(CH_2)_2$, $ZrH_3-CH=CH_2$, and $ZrH_2=CHCH_3$ optimized at the level of B3LYP/6-311++G-(3df,3pd)/SDD. The bond lengths and angles are in Å and deg. The Zr metallacyclopropane dihydride ($ZrH_2-(CH_2)_2$(S)) is 6.0, 4.2, and 20 kcal/mol more stable than $ZrH-CH_2CH_3$(T), $ZrH_3-CH=CH_2$(S), and $ZrH_2=CHCH_3$(S), respectively. $ZrH-CH_2CH_3$, $ZrH_2-(CH_2)_2$, and $ZrH_3-CH=CH_2$ are identified in the IR spectra shown in Figures 1 and 2.

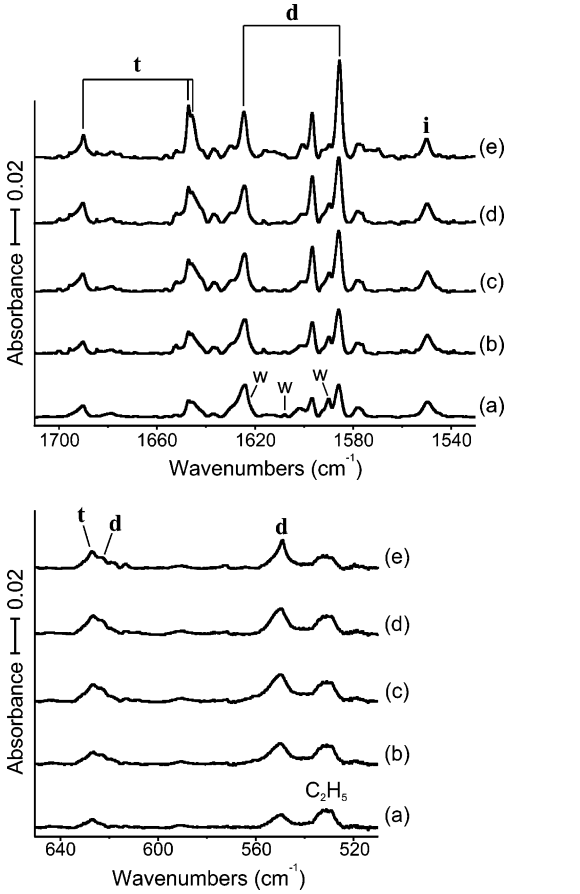

Figure 5. IR spectra in the regions of 1710−1530 and 650−510 cm^{-1} for laser-ablated Hf atoms co-deposited with C_2H_6 in excess argon at 8 K. (a) Hf + 1.0% C_2H_6 in Ar co-deposited for 1 h. (b) As in a after photolysis ($\lambda > 420$ nm). (c) As in b after photolysis ($240 < \lambda < 380$ nm). (d) As in c after photolysis ($\lambda < 220$ nm). (e) As in d after annealing to 28 K. **i**, **d**, and **t** denote the product absorption groups, and w indicates water residue absorption.

On the other hand, group 6 trihydrides form readily in the reaction with methane.[14−16]

Another conceivable product is the C−C insertion complex, $Zr-(CH_3)_2$, which is only 6.0 kcal/mol higher than $ZrH_2-(CH_2)_2$. However, Carroll et al. investigated gas-phase reactions of second-row transition metals with small hydrocarbons and reported that the activation energy for C−C insertion is expected to be about 20 kcal/mol higher than that for C−H insertion.[17] Calculations also show that the vibrational bands are predicted to be very weak, except for the antisymmetric $Zr-C_2$ stretching absorption, which is expected at about 450 cm^{-1}, considering the scale factor. No absorption can be assigned to the C−C insertion product in this study.

Although gas-phase ground-state Zr atoms were unreactive with ethane,[17] the present matrix isolation investigation employs excited Zr atoms through the laser ablation process and subsequent UV irradiation. Hydrogen elimination, important in other gas-phase metal atom reactions,[17] is not in the matrix reactions presumably owing to matrix quenching of energized reaction products. We note that none of the $Zr(C_2H_4)$ reaction products[27] were observed in the ethane experiments, and this would be logical for H_2 elimination products.

The structures of $ZrH-CH_2CH_3$, $ZrH_2-(CH_2)_2$, ZrH_3-CCH_3, and $ZrH_2=CHCH_3$ with C_1, C_{2v}, C_s, and C_s symmetries, respectively, are shown in Figure 4. The insertion product has a triplet ground state, but all others have a singlet ground state. $ZrH-CH_2CH_3$(T), $ZrH_2-(CH_2)_2$(S), ZrH_3–CCH_3(S), and $ZrH_2=CHCH_3$(S) are 25, 48, 44, and 28 kcal more stable than $Zr(^3F_2) + C_2H_6$. As described above and suggested by previous studies,[17] the metal atom + ethane reaction is believed to proceed following the reaction path.

$$Zr^*(^3F) + C_2H_6 \rightarrow H-Zr-CH_2CH_3^* \rightarrow ZH_2-(CH_2)_2^* \rightarrow ZrH_3-CCH_3$$

Intersystem crossing then must occur somewhere on the pathway. The relative energies (Figure 3) suggest that the lowest energy intersystem crossing transition would be to the singlet TS, leading to the most stable metallacycle product.

Hf + C_2H_6. Figures 5 and 6 illustrate IR spectra from the reactions of Hf atoms with ethane and their variations on photolysis and annealing. The original Hf + C_2H_6 spectra are similar to the Zr + C_2H_6 spectra shown in Figures 1 and 2, except for the fact that the **i** and **t** absorptions are relatively weaker and stronger in the Hf−H stretching region, respectively. The observed frequencies are summarized in Table 2. The intensity changes on photolysis are relatively smaller. The **i** absorptions increase about 10% on visible irradiation and increase another 5% on the following UV irradiation. The **i** absorptions show essentially no further changes in intensity in the subsequent photolysis. The **d** absorptions increase ~30% and ~40% on the first visible and subsequent UV photolysis. They further increase slightly in the following full arc ($\lambda >$ 220 nm) and second visible photolysis. The **t** absorptions increase slightly on visible photolysis but show ~40% increases on UV photolysis and slight growth on the subsequent full arc photolysis.

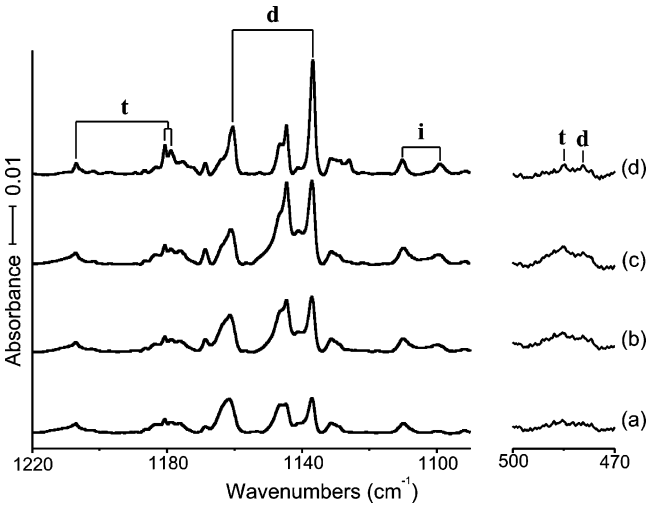

Figure 6. IR spectra in the regions of 1220−1090 and 500−470 cm^{-1} for laser-ablated Hf atoms co-deposited with C_2D_6 in excess argon at 8 K. (a) Hf + 1.0% C_2D_6 in Ar co-deposited for 1 h. (b) As in a after photolysis (λ > 420 nm). (c) As in b after photolysis (240 < λ < 380 nm). (d) As in c after annealing to 28 K. **i**, **d**, and **t** denote the product absorption groups.

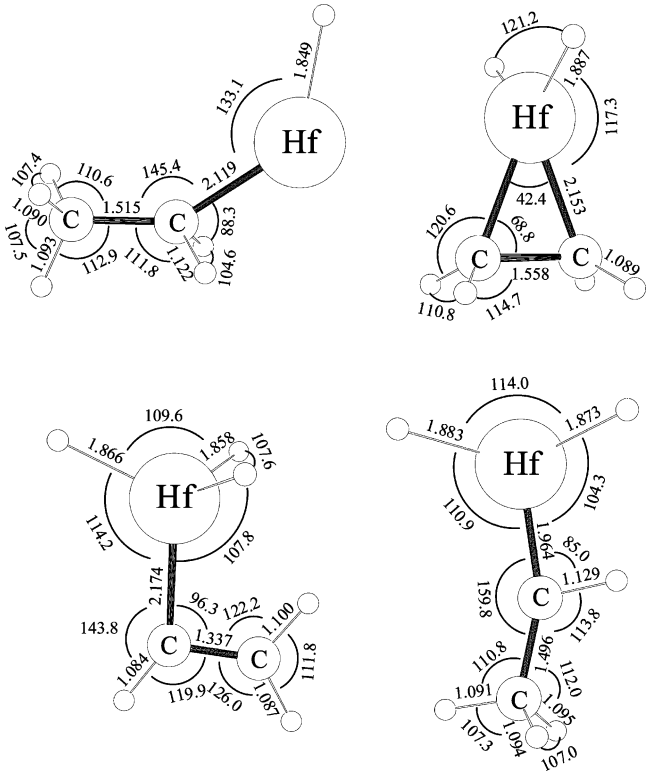

Figure 7. Structures of HfH−CH_2CH_3, HfH_2−$(CH_2)_2$, HfH_3−CH═CH_2, and HfH_2═$CHCH_3$ optimized at the level of B3LYP/6-311++G-(3df,3pd)/SDD. The bond lengths and angles are in Å and deg. The Hf metallacyclopropane dihydride (HfH_2−$(CH_2)_2$(S)) is 26, −1.2, and 22 kcal/mol more stable than HfH−CH_2CH_3(T), HfH_3−CH═CH_2(S), and HfH_2═$CHCH_3$(S), respectively. HfH−CH_2CH_3, HfH_2−$(CH_2)_2$, HfH_3−CH═CH_2, and HfH_2═$CHCH_3$ have C_s, C_{2v}, C_s, and C_1 structures. HfH−CH_2CH_3, HfH_2−$(CH_2)_2$, and HfH_3−CH═CH_2 are identified in the IR spectra shown in Figures 3 and 4.

Previous studies show that the hydrogen stretching frequencies of hafnium hydrides tend to increase with the number of Hf−H bonds, and no stretching absorptions of binary hafnium hydrides (Hf_xH_y) are observed in this study.[29] Parallel to the Zr + C_2H_6 system, the **i**, **d**, and **t** absorptions in the Hf + C_2H_6 spectra are attributed to mono-, di-, and trihydrido products,

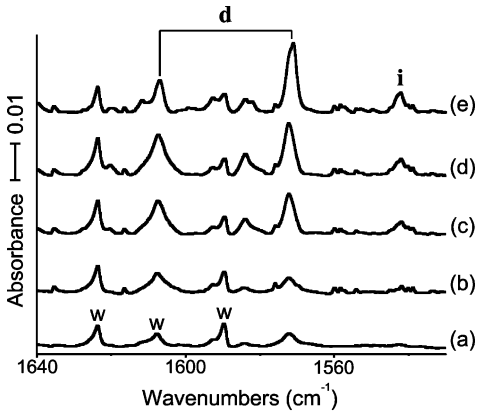

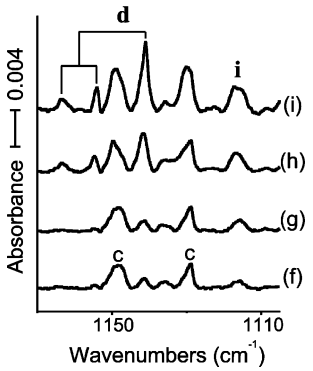

Figure 8. Ti−H and Ti−D stretching regions for the product of laser-ablated Ti atom reaction with C_2H_6 and C_2D_6 in excess argon. (a) Ti + 1.0% C_2H_6 in Ar co-deposited for 1 h. (b) As in a after photolysis (λ > 420 nm). (c) As in b after photolysis (240 < λ < 380 nm). (d) As in c after photolysis (λ < 220 nm). (e) As in d after annealing to 28 K. (f) Ti + 1.0% C_2D_6 in Ar co-deposited for 1 h. (g) As in f after photolysis (λ > 420 nm). (h) As in g after photolysis (λ < 220 nm). (i) As in h after annealing to 28 K. **i**, **d**, and **t** denote the product absorption groups, and w and c indicate water and common absorptions.

respectively. The **i** absorption at 1549.8 cm^{-1}, which is much weaker relative to the Zr case, has its deuterium counterpart at 1110.0 cm^{-1} (H/D ratio of 1.396), and we assign the single Hf−H stretching band to the Hf−H stretching mode of HfH−CH_2CH_3. The observed frequencies are in reasonable agreement with the predicted values as shown in Tables 2 and S5. No other **i** absorptions are observed, which is traced to the low absorption intensities of the vibrational bands predicted for the insertion complex other than the Hf−H stretching band as shown in Table S5.

Parallel to the Zr + C_2H_6 system, the **d** absorptions at 1624.4 and 1585.8 cm^{-1} appear prominent in the hydrogen stretching region. The D counterparts are observed at 1161.0, 1144.6, and 1137.1 cm^{-1} (H/D ratios of 1.399, 1.395, and 1.395). The frequencies are compared with the previously reported Hf−H stretching frequencies of 1622.4, 1646, and 1683.2 cm^{-1} for HfH_2, HfH_3, and HfH_4 and Hf−D stretching frequencies of 1161.0, 1180.2, and 1205.4 cm^{-1} for HfD_2, HfD_3, and HfD_4, respectively.[29]

The **d** absorptions in the Hf−H stretching region suggest a reaction product with a HfH_2 group, and the most plausible ones are again metallacyclic and methylidene complexes, HfH_2−$(CH_2)_2$ and HfH_2═$CHCH_3$. Similar to the Zr + C_2H_6 case, the metallacyclic complex is 22 kcal/mol more stable than the methylidene product, and the observed vibrational characteristics are in a better agreement with those of the cyclic complex. A **d** absorption and its D counterpart are observed at 623.0 and 479.6 cm^{-1} (H/D ratios of 1.299), and they are assigned to the

TABLE 2: Observed and Calculated Harmonic Frequencies of Product Absorptions from Reactions of Ethane with Hf in Excess Argon[a]

	C_2H_6		C_2D_6		
	obsd	calcd	obsd	calcd	description
i	1549.8	1666.0 (380)	1110.0	1173.4 (127)	Hf−H str.
d	1624.4	1656.7 (339)	1161.0	1173.6 (172)	A_1 HfH_2 str.
	623.0	651.7 (83)	479.6	483.4 (64)	A_1 HfH_2 scis.
	1596.6, 1585.8	1619.3 (618)	1144.6, 1137.1	1151.1 (314)	B_1 HfH_2 str.
	550.2	549.9 (105)		478.4 (71)	B_2 HfC_2 str.
t	1690.3	1726.0 (207)	1207.1	1222.1 (106)	A HfH_3 str.
	1645.8	1679.7 (504)	1178.9	1192.8 (257)	A HfH_3 str.
	1207.7	1242.9 (14)		1023.1 (7)	A HCHf bend
	885.9	921.8 (15)		669.5 (8)	A CH_2 rock
	626.9	622.3 (244)	485.4	509.2 (102)	A HfH_3 deform
	1647.3	1683.0 (459)	1180.6	1195.6 (235)	A HfH_3 str.
	460.9	468.7 (68)		354.8 (37)	A HfH_3 rock

[a] All frequencies are in cm^{-1}. Observed in argon matrix; stronger absorptions are bold. Description gives major coordinate. **i**, **d**, and **t** stand for insertion, dihydrido, and trihydrido products, respectively. Harmonic frequencies calculated with B3LYP/6-311++G(3df,3pd)/SDD are not scaled.

TABLE 3: Observed and Calculated Harmonic Frequencies of Product Absorptions from Reactions of Ethane with Ti in Excess Argon[a]

	C_2H_6		C_2D_6		
	obsd	calcd	obsd	calcd	description
i	1542.3	1573.7 (422)	1115.8	1122.3 (175)	Ti−H str.
d	1607.5	1672.9 (407)	1163.4, 1154.6	1191.5 (185)	A_1 TiH_2 str.
	1010.6	1077.5 (40)		902.0 (19)	A_1 CC str.
	600.6	661.1 (72)		515.6 (30)	A_1 TiH_2 scis.
	1572.2	1633.4 (651)	1141.7	1175.4 (340)	B_1 TiH_2 str.
	503.0	508.4 (134)		439.4 (84)	B_2 TiC_2 str.

[a] Frequencies are in cm^{-1}; observed in argon matrix; calculated using B3LYP and not scaled. Description gives major coordinate. **i** and **d** indicate insertion and methylidene products, respectively.

A_1 HfH_2 scissoring mode of the cyclic complex. Another **d** absorption at 550.2 cm^{-1} is designated to the B_2 HfC_2 stretching modes, and the D counterpart is probably covered by the broad absorption feature at about 480 cm^{-1}. On the basis of the stability and agreement between observed and predicted vibrational characteristics, we assign the **d** absorptions to the metallacyclic product, $HfH_2-(CH_2)_2$, parallel to the Zr system.

The **t** absorptions at 1690.3, 1647.3, and 1645.8 cm^{-1} have the D counterparts at 1207.1, 1180.6, and 1178.9 cm^{-1} (H/D ratios of 1.400, 1.395, and 1.396), respectively. The Hf−H stretching absorptions are much stronger relative to those in the Zr + C_2H_6 spectra in Figures 1 and 2. The relatively high Hf−H stretching frequencies suggest a reaction product with a HfH_3 group responsible for the **t** absorptions, and $HfH_3-CH=CH_2$ is energetically the most probable, which is 1.2 and 22 kcal/mol more stable than $HfH_2-(CH_2)_2$ and $HfH-CH_2CH_3$ in the singlet ground states, respectively. Another **t** absorption and its D counterpart are observed at 626.9 and 485.4 cm^{-1}, respectively, and they are assigned to the HfH_3 deformation mode, whose intensity is predicted to be much stronger than those of other low-frequency absorptions as shown in Table S7.

Weak **t** absorptions are also observed at 1207.7, 885.9, and 460.9 cm^{-1} (not shown), and they are tentatively assigned to the A′ H−C−Hf bending, A′ CH_2 rocking, and A″ HfH_3 rocking modes of the trihydrido product without observation of the D counterparts. Figure 7 shows the structures of $HfH-CH_2CH_3$, $HfH_2-(CH_2)_2$, $HfH_3-CH=CH_2$, and $HfH_2=CHCH_3$ with C_s, C_{2v}, C_s, and C_1 symmetries. They all have a singlet ground state and are 26, 46, 47, and 24 kcal/mol more stable than the reactants, $Hf(^3F_2)$ + C_2H_6. Like previously studied small Hf complexes, the C−Hf bond lengths are mostly shorter than those of the corresponding Zr products and the Hf−H and C−Hf stretching frequencies are also higher owing to the effects of relativistic contraction.[12,13,29,31] The lower energy of the trihyrido complex ($HfH_3-CH=CH_2$) explains the high yield of the higher oxidation-state product relative to the Zr compound.

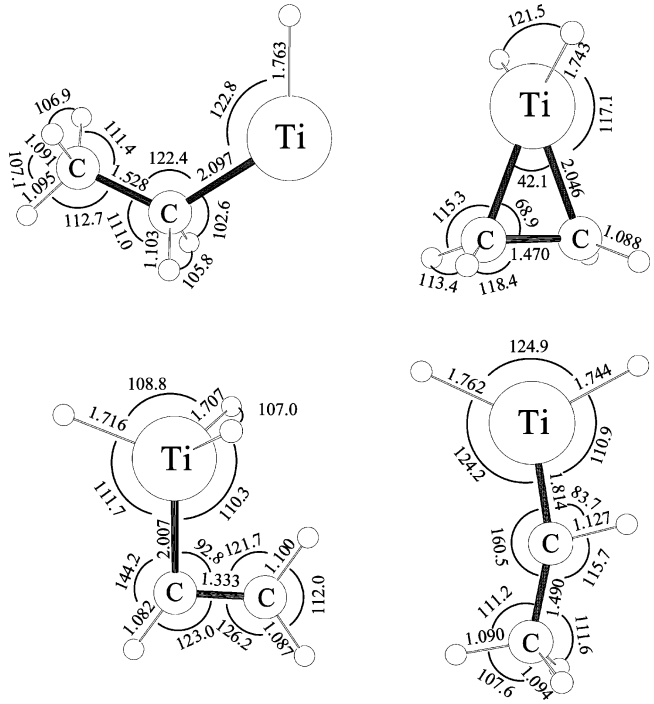

Figure 9. Structures of $TiH-CH_2CH_3$, $TiH_2-(CH_2)_2$, $TiH_3-CH=CH_2$, and $TiH_2=CHCH_3$ optimized at the level of B3LYP/6-311++G(3df,-3pd). The all-electron basis is used for Ti. The bond lengths and angles are Å and deg. The Ti metallacyclopropane dihydride ($TiH_2-(CH_2)_2$-(S)) is 5.0, 16, and 21 kcal/mol more stable than $TiH-CH_2CH_3$(T), $TiH_3-CH=CH_2$(S), and $TiH_2=CHCH_3$(S), respectively. $TiH-CH_2CH_3$, and $TiH_2-(CH_2)_2$ are identified in the IR spectra shown in Figure 8.

Ti + C_2H_6. Shown in Figure 8 are the Ti−H stretching regions in the IR spectra from reactions of laser-ablated Ti atoms with ethane. Titanium is the least reactive with ethane based on the product absorption intensities. The product bands are marked with **i** and **d** following the Zr and Hf cases, and their frequencies are summarized in Table 3. The observed frequencies are compared with the previously reported Ti−H stretching frequencies of 1435.5, 1580.6, and 1663.8 cm^{-1} for TiH_2, TiH_3, and TiH_4 and Ti−D stretching frequencies of 1041.0, 1147.2, and 1205.6 cm^{-1} for TiD_2, TiD_3, and TiD_4. These binary titanium hydride absorptions[32] are not observed in this study.

The product absorptions increase slightly on visible photolysis, but they triple on the subsequent UV irradiation. The single **i** absorptions and the D counterpart at 1542.3 and 1115.8 cm^{-1} (H/D ratio of 1.382), respectively, are attributed to the Ti−H stretching mode of $TiH-CH_2CH_3$. The **d** absorptions at 1607.5 and 1572.2 cm^{-1} have D counterparts at 1154.6 and 1148.8 cm^{-1} (1.392 and 1.398) with a roughly 1:2 ratio in intensity. We assign the **d** absorptions to the Ti−H stretching modes of $TiH_2-(CH_2)_2$ in line with the Zr and Hf reactions. In the low-frequency region, weak and broad absorption features are observed at 600.6 and 503.0 cm^{-1} (not shown) and tentatively assigned to the A_1 TiH_2 scissoring and B_2 TiC_2 stretching mode without observation of the D counterparts.

The **t** absorptions are not observed in the IR spectra of Ti + C_2H_6, unlike the Zr and Hf systems. Calculations show that while $TiH-CH_2CH_3$(T) and $TiH_2-(CH_2)_2$(S) are 17 and 22 kcal/mol more stable than $Ti(^3F_2) + C_2H_6$, $TiH_2=CHCH_3$(S) and $TiH_3-CH=CH_2$(S) are only 1.5 and 6.2 kcal/mol more stable than the reactants. As a result, the trihydrido product is much less favored in the reaction of Ti + C_2H_6 in comparison with the Zr and Hf cases. Shown in Figure 9 are the structures of $TiH-CH_2CH_3$(T), $TiH_2-(CH_2)_2$(S), $TiH_3-CH=CH_2$(S), and $TiH_2=CHCH_3$(T) with C_s, C_{2v}, C_s, and C_s symmetries.

Conclusions

Reactions of laser-ablated group 4 metal atoms with ethane were investigated, and the matrix IR spectra and variation on photolysis and annealing were examined. Three sets of product absorptions were observed for major reaction products: the insertion complex ($MH-CH_2CH_3$), the cyclic dihydrido complex ($MH_2-(CH_2)_2$), and the trihydrido complex ($MH_3-CH=CH_2$). Particularly, the observed strong metal−hydrogen stretching absorptions show that C−H insertion and subsequent reactions readily occur for group 4 metal atoms with ethane, which is consistent with the previous results from reactions of metal atoms with methane and methyl halides.[14]

The insertion complex is believed to form first in reaction of metal atoms with ethane and following hydrogen migrations leads to the dihydrido and trihydrido products. In particular, formation of the dihydrido cyclic product involves β-hydrogen migration. Not only is the dihydrido cyclic complex more stable than the methylidene complex ($MH_2=CHCH_3$), but the transition state to the product is predicted to be more stable as well. The reaction yield for $MH_3-CH=CH_2$ varies substantially with the metal: it is highest with Hf and too low with Ti to identify the product. The variation in reaction yield is traced to the stability of the product: the Hf and Ti trihydrido complexes are the most and least stable among the major products.

Acknowledgment. We gratefully acknowledge support for this research from the National Science Foundation under Grant No. CHE03-52487.

Supporting Information Available: Tables of calculated frequencies. This material is available free of charge via the Internet at http://pubs.acs.org.

References and Notes

(1) Crabtree, R. H. *Chem. Rev.* **1995**, *95*, 987 and references therein.
(2) Grubbs, R. H.; Coates, G. W. *Acc. Chem. Res.* **1996**, *29*, 85.
(3) Choi, S.-H.; Lin, Z. *Organometallics* **1999**, *18*, 5488.
(4) Buchmeiser, M. R. *Chem. Rev.* **2000**, *100*, 1565.
(5) Schrock, R. R. *Chem. Rev.* **2002**, *102*, 145.
(6) Ujaque, G.; Cooper, A. C.; Maseras, F.; Eisenstein, O.; Caulton, K. G. *J. Am. Chem. Soc.* **1998**, *120*, 361.
(7) Wada, K.; Craig, B.; Pamplin, C. B.; Legzdins, P.; Patrick, B. O.; Tsyba, I.; Bau, R. *J. Am. Chem. Soc.* **2003**, *125*, 7035.
(8) Clot, E.; Eisenstein, O. Agostic Interactions from a Computational Perspective. *Structure and Bonding, Computational Inorganic Chemistry*; Kaltzoyannis, N., McGrady, E., Eds.; Springer-Verlag: Heidelberg, 2004; pp 1−36.
(9) Scherer, W.; McGrady, G. S. *Angew. Chem., Int. Ed.* **2004**, *43*, 1782.
(10) Roos, B. O.; Lindh, R. H.; Cho, H.-G.; Andrews, L. *J. Phys. Chem. A* **2007**, *111*, 6420 (theoretical study of $CH_2=MH_2$ complexes).
(11) Andrews, L.; Cho, H.-G.; Wang, X. *Inorg. Chem.* **2005**, *44*, 4834 (Ti + CH_4).
(12) (a) Andrews, L.; Cho, H.-G.; Wang, X. *Angew. Chem., Int. Ed.* **2005**, *44*, 113. (b) Cho, H.-G.; Wang, X.; Andrews, L. *J. Am. Chem. Soc.* **2005**, *127*, 465 (Zr + CH_4).
(13) Cho, H.-G.; Wang, X.; Andrews, L. *Organometallics* **2005**, *24*, 2854 (Hf + CH_4).
(14) Andrews, L.; Cho, H.-G. *Organometallics* **2006**, *25*, 4040 (review article).
(15) Cho, H.-G.; Andrews, L. *J. Am. Chem. Soc.* **2005**, *127*, 8226 (Mo + CH_4).
(16) Cho, H.-G.; Andrews, L.; Marsden, C. *Inorg. Chem.* **2005**, *44*, 7634 (W + CH_4).
(17) Carroll, J. J.; Haug, K. L.; Weisshaar, J. C.; Blomberg, M. R. A.; Siegbahn, Per, E. M.; Svensson, M. *J. Phys. Chem.* **1995**, *99*, 13955.
(18) Andrews, L.; Citra, A. *Chem. Rev.* **2002**, *102*, 885 and references therein.
(19) Andrews, L. *Chem. Soc. Rev.* **2004**, *33*, 123 and references therein.
(20) Kudin, K. N., et al. *Gaussian 03*, revision B.04; Gaussian, Inc.: Pittsburgh, PA, 2003.
(21) (a) Becke, A. D. *J. Chem. Phys.* **1993**, *98*, 5648. (b) Lee, C.; Yang, Y.; Parr, R. G. *Phys. Rev. B* **1988**, *37*, 785.
(22) Frisch, M. J.; Pople, J. A.; Binkley, J. S. *J. Chem. Phys.* **1984**, *80*, 3265.
(23) (a) Wachters, A. J. H. *J. Chem. Phys.* **1970**, *52*, 1033. (b) Hay, P. J. *J. Chem. Phys.* **1977**, *66*, 4377.
(24) Andrae, D.; Haeussermann, U.; Dolg, M.; Stoll, H.; Preuss, H. *Theor. Chim. Acta* **1990**, *77*, 123.
(25) Page, M.; Doubleday, C.; McIver, J. W., Jr. *J. Chem. Phys.* **1990**, *93*, 5634.
(26) Frisch, M. J.; Head-Gordon, M.; Pople, J. A. *Chem. Phys. Lett.* **1990**, *166*, 281.
(27) Cho, H.-G.; Andrews, L. J. *Phys. Chem. A* **2004**, *108*, 3965−3972 (Zr + C_2H_4).
(28) (a) Chettur, C.; Snelson, A. J. Phys. Chem. **1987**, *91*, 3483. (b) Jacox, M. E. *J. Phys. Chem. Ref. Data* **1995**, *99*, 323.
(29) Chertihin, G. V.; Andrews, L. *J. Phys. Chem.* **1995**, *99*, 15004 (Zr and Hf + H_2).
(30) (a) Scott, A. P.; Radom, L. *J. Phys. Chem.* **1996**, *100*, 16502. (b) Andersson, M. P.; Uvdal, P. L. *J. Phys. Chem. A* **2005**, *109*, 3937.
(31) Pyykko, P. *Chem. Rev.* **1988**, *88*, 563.
(32) Chertihin, G. V.; Andrews, L. *J. Am. Chem. Soc.* **1994**, *116*, 8322 (Ti + H_2).